

Theoretical Modelling of Portable Vertical Axis Wind Harvesting System

Lew Heng Loong¹, Kok Boon Ching^{1*}

¹Faculty of Electrical and Electronic Engineering,
Universiti Tun Hussein Onn Malaysia, 86400 Parit Raja, Johor, MALAYSIA

*Corresponding Author Designation

DOI: <https://doi.org/10.30880/eeee.2021.02.02.106>

Received 04 July 2021; Accepted 11 October 2021; Available online 30 October 2021

Abstract: As the depletion of fossil-fuel resources is exacerbated due to the increasing power demand of industries and transportation, harnessing wind energy is essential to replace non-renewable energy in generating energy. Moreover, the low annual wind speed in Malaysia is one of the factors that increases the difficulty of harnessing wind energy in generating electrical energy. In this paper, a portable vertical axis wind energy harvesting system (VAWEHS) that can extract energy from wind with low speed is presented for the application of high-rise buildings. Savonius wind turbine which is a type of vertical axis wind turbine (VAWT) is modelled based on related equation in converting wind energy to electrical energy, and the performance of system is further enhanced by permanent magnet DC generator (PMDCG), boost converter, bidirectional converter, and DC-link voltage control scheme. In MATLAB/SIMULINK simulation with a duration of 100 seconds, the proposed VAWEHS can provide a maximum output voltage of 18.5 across a 10.8 load and store a portion of electrical energy into a lead-acid battery under wind speeds of 1.667 m/s, 2.500 m/s, 3.611 m/s, 5.278 m/s, and 6.667 m/s. It is also capable to supply a current of 1.7A at the voltage of 18.5 V with the help of boost converter during the discharging process. It is concluded that the proposed design of VAWEHS can perform well in generating electrical energy by harnessing wind energy. In future, the system can be further improved by introducing advanced control schemes

Keywords: Renewable Energy, Portable Vertical Axis, Wind Harvesting System, Wind Turbine

1. Introduction

As the depletion of the fossil-fuel resources becomes worse due to the increasing demand on power for industries and transportation, harnessing wind energy is an alternative solution to replace non-renewable resource in generating electrical energy. Renewable energy (RE) is a type of energy that is produced from natural resources, which can be constantly replenished [1]. Sun, ocean tides, wind, rain, geothermal resources, and biomass are the examples of renewable energy in this world. In

*Corresponding author: bckok@uthm.edu.my

2021 UTHM Publisher. All rights reserved.

publisher.uthm.edu.my/periodicals/index.php/eeee

Malaysia, more than 90% of electricity generated was attained from fossil fuel [2]. The combustion of fossil-fuel may emit high levels of air pollutants that are harmful to both environment and public health. Apart from solar energy, wind energy is found that has the potential to be the main resource in generating electrical energy. This is because Malaysia experiences two main weather seasons that are southwest monsoon from May or June to September and northeast monsoon from November to March [3]. In 2007, a new energy harvesting system that features a wind turbine, and hybrid solar, generator, and battery was built in Pulau Perhentian, Terengganu [4]. This evidence showed the possibility of harnessing wind energy to generate electrical energy in Malaysia.

The mean annual wind speed in Malaysia is considerably low at 2 m/s and it does not blow uniformly as Malaysia experience stronger winds in the early and late parts of the year [3]. Due to this phenomenon, harnessing wind energy in Malaysia is said to be challenging and difficult in Malaysia. Besides, an energy harvesting system will be merited if it can store electrical storage into a battery storage. This feature is beneficial to an emergency like a blackout. In this study, it is hypothesised that a VAWT is a suitable design in producing a greater amount of electrical power generated at the output terminal. This study is also focus on the relationship between the speed of wind and the amount of electrical energy generated from the wind energy harvesting system (WEHS).

Therefore, a portable VAWEHS that can extract as much energy from the wind as possible throughout a range of wind speed is proposed. Besides, power management system that can store a portion of electrical energy into battery storage is also designed for the proposed VAWEHS. Several scopes are covers in this paper. The proposed VAWEHS is designed to be applied for high-rise buildings and composed of VAWT for single-phase application. The conversion of wind energy to electrical energy is derived theoretically based on literature reviews and the VAWT is modelled based on the equations derived in this paper.

2. Methodology

This section will present the methodologies used in developing the proposed portable VAWEHS. The first subsection presents the equations used in modelling the VAWTs. The second subsection presents the flow chart of process in designing the proposed VAWEHS.

2.1 Equations

A VAWT is an aerodynamic model that can extract power from the wind in the form of kinetic energy before it is converted into mechanical energy and fed to the generator. In this paper, the modelling of the VAWT is done based on the equations in this subsection. The mechanical power produced by VAWT, P_m is expressed as

$$P_m = \frac{1}{2} C_{p(\lambda)} \rho A v^3 \quad Eq. 1$$

where ρ is the density of air which is known as 1.225 kg/m³ at normal temperature, v is the speed of wind in meter per second, and C_p is the power coefficient of the wind turbine, λ is the tip-speed ratio, and A is the wind turbine swept area that can be calculated as [5].

$$A = 2RH \quad Eq. 2$$

where H is the height of the wind turbine blade in meter, and R is the rotor radius of the wind turbine in meter. In order to calculate the power coefficient of the wind turbine, C_p , is calculated by using a generic equation that is expressed as [5]

$$C_p(\lambda, \theta) = 0.22 \left(\frac{116}{\lambda_i} - 0.4\theta - 5 \right) e^{\left(\frac{12.5}{\lambda_i} \right)} + 0.0068\lambda_i \quad \text{Eq. 3}$$

where λ_i is the value of tip-speed ratio for a particular pitch angle, and θ is the pitch angle of wind turbine. The value of λ_i can be determined by using the equation shown as below [5]

$$\frac{1}{\lambda_i} = \frac{1}{\lambda + 0.08\theta} - \frac{0.035}{1 + \theta^3} \quad \text{Eq. 4}$$

where λ is the tip speed ratio that is defined as the ratio of the rotating blade tip to the speed of free wind stream. In this case, the tip speed ratio can be optimised by using the value of the number of turbine blades into the equation as below [6]

$$\lambda_{opt} = \frac{4\pi}{B} \quad \text{Eq. 5}$$

where B is the number of turbine blades. With the aid of VAWT, mechanical torque T_m can be produced and sent to generators as their driving force to generate electrical energy. The relationship between the mechanical torque, T_m and mechanical power, P_m can be expressed as [7]

$$T_m = \frac{P_m}{\omega_m} \quad \text{Eq. 6}$$

where ω_m is the rotor angular speed. The relationship between the rotor angular speed ω_m in $rads^{-1}$ and the tip-speed ratio is given as [5]

$$\omega_m = \frac{\lambda_{opt} v}{R} \quad \text{Eq. 7}$$

However, the mechanical torque is in the unit of $Watt / rads^{-1}$. According to the manual written by Andrew Russakoff [8], mechanical torque in the unit of $Watt / rads^{-1}$ can be converted to Nm by using the formula below

$$T_m (Nm) = T_m (Watt / rads^{-1}) \div CF \quad \text{Eq. 8}$$

where CF is a conversion factor which is represented by a value of 1.0002. By substituting mechanical power P_m from Eq.1 and rotor angular speed ω_m from Eq.7 into Eq.6, the formula of mechanical torque can be simplified as below [5]

$$T_m = \frac{1}{2} C_t \rho A R v^2 \quad \text{Eq.9}$$

where C_t is the torque coefficient of the wind turbine and it can be expressed as [5]

$$C_t = \frac{C_p}{\lambda} \quad \text{Eq. 10}$$

2.2 Methods

MATLAB/SIMULINK 2018b is used to simulate the proposed VAWEHS. Modelling of VAWT is carried out according to the equations in the previous subsection. The purpose of modelling the VAWT is to exhibit the characteristics of capturing the wind from all direction as the Savonius wind turbine. The procedures in modelling the VAWT is shown in Figure 1. After the model of VAWT is

developed, the mechanical torque signal of the VAWT is connected to the PMDFG so that mechanical power of wind turbine can be converted to electrical energy.

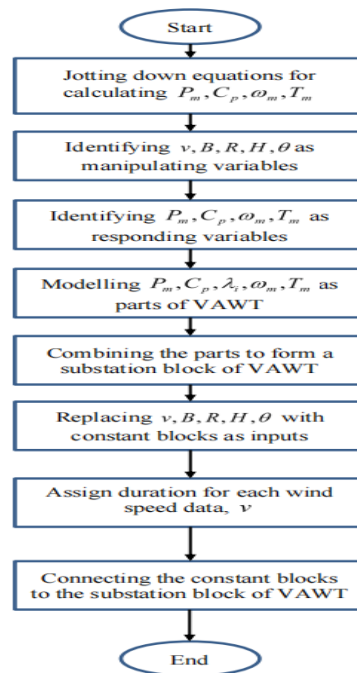


Figure 1: The procedures in modelling VAWT

Besides, boost converter is needed to boost the voltage across the output terminal to the desired level. Before designing the boost converter, the design requirement of the boost converter must be fixed first. Next, the duty cycle, minimum value of inductance and capacitance of the boost converter are determined after fixing the design requirement. The flow chart of procedures in designing the boost converter is shown in Figure 2.

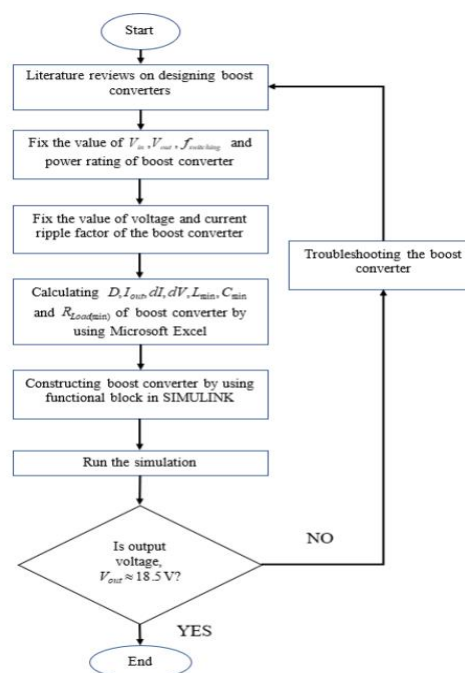


Figure 2: The procedures in designing the boost converter

To store the electrical energy into the lead-acid battery, a bidirectional converter (BDC) is required. Similar to the designing of boost converter, the design requirement of the BDC must be decided before determining its other parameters such as duty cycle, minimum inductance and minimum capacitance. Figure 3 shows the flow chart of methods used in designing the BDC.

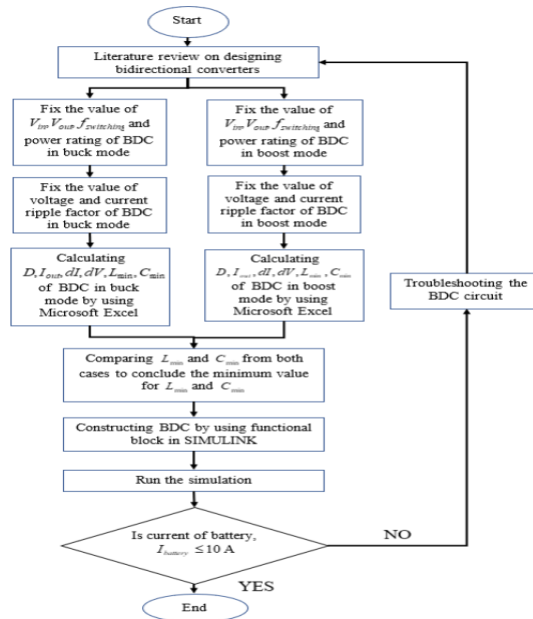


Figure 3: The flow chart of methods used in designing BDC

Lastly, as the wind speed is varied according to simulation time, the output voltage will not be at the desired level. To overcome this problem, DC-link voltage control scheme is introduced as the control scheme used in controlling the duty cycle of the boost converter and BDC. By using DC-link voltage control scheme, the output voltage will be compared with a reference value and the error between these two values will be fed to a P controller. Therefore, the duty cycle of the converter can be changed from time to time in order to stabilise the voltage across the output terminal. Figure 4 shows the flow of processes in designing the DC-link voltage control scheme.

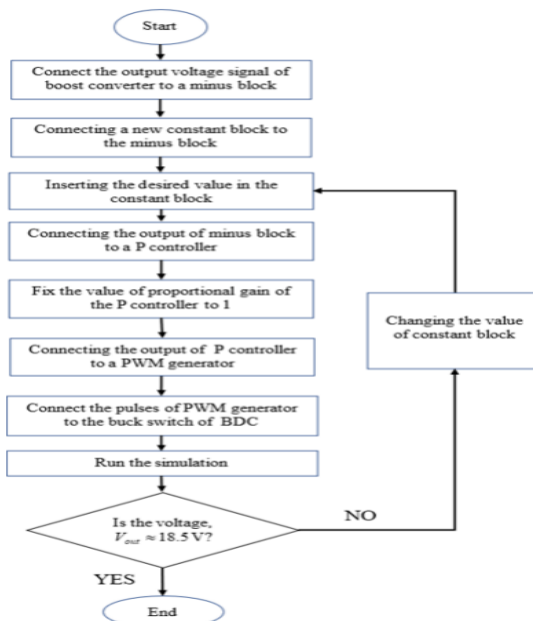


Figure 4: The flow of processes in designing the DC-link voltage control scheme

3. Results and Discussions

The results that have been obtained throughout this study are analysed and explained in this section. The proposed VAWEHS is simulated for 100 seconds, and various results are analysed after they are plotted.

3.1 Mechanical power, angular speed, and mechanical torque of a VAWT (charging process)

Theoretically, the mechanical power, rotor angular speed, and mechanical torque of a VAWT are determined by the wind speed. The wind speed is increased to other level of magnitude after every 20 seconds and its graph is shown in Figure 5. Figure 6 to Figure 8 show the graphs of mechanical power, rotor angular speed, and mechanical torque of a VAWT, respectively. Based on those figures, increments are shown in mechanical power, rotor angular speed and mechanical torque when the wind speed is increased during the simulation.

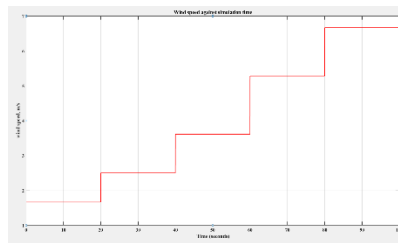


Figure 5: The graph of wind speed against simulation time

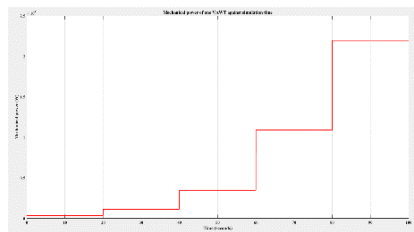


Figure 6: The graph of mechanical power against simulation time

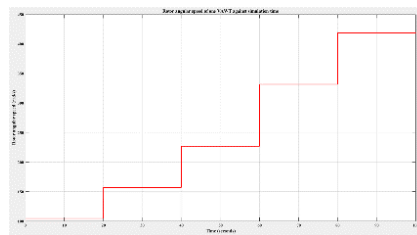


Figure 7: The graph of rotor angular speed against simulation time

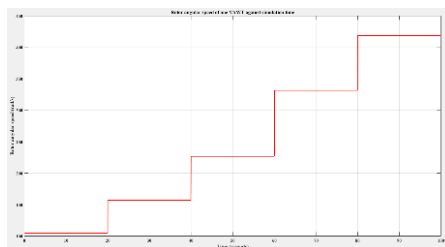


Figure 8: The graph of mechanical torque against simulation time

3.2 Stator current and rotor speed of a PMDCG (charging process)

Figure 9 and Figure 10 show the graphs of rotor speed and armature current of a PMDCG against simulation time, respectively. From Figure 9, the rotor speed of the PMDCG is able to achieve stability after a very short period of time. This phenomenon enables the stability of the armature current can be achieved also since the armature current is affected by the rotor speed of the PMDCG. Negative value can be found from the graph of armature current because the current flows out from the generator. Then, the current will be sent to the boost converter so that it can boost the voltage of 18.5V across the load with $10.8\ \Omega$.

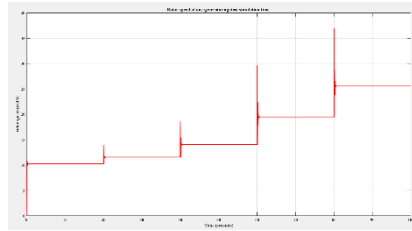


Figure 9: The graph of rotor speed against simulation time

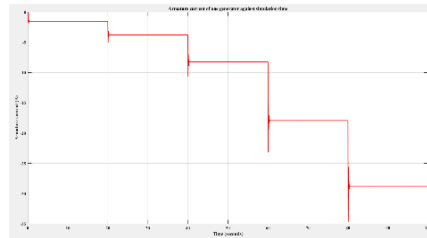


Figure 10: Graph of armature current against simulation time

3.3 Input DC-link voltage, output dc-link voltage and output current of boost converter (charging process)

The boost converter is designed so that the voltage across a load with $10.8\ \Omega$ can be maintained at 18.5 V. Figure 11 shows the graph of input DC-link voltage against simulation time. The function of input capacitance is to stabilise the input voltage and protect it from ripple voltage. From Figure 12, the input voltage across the input capacitor is maintained at the level of 17.1 V. This can be achieved also by fixing the duty cycle of the signal which control the switching device of boost converter to 0.15. The input capacitor of the boost converter must be highly charged in order to provide a portion of current to the battery for charging purpose. The fluctuations of the waveform are caused by the change in speed of wind. Similar to the previous explanation, the rotor speed of the PMDCG need time to achieve stability. Figure 12 and Figure 13 show the graph of output voltage and output current of boost converter. From both figures, the boost converter is able to maintain the output voltage to 18.5 V and supply a current of 1.7 A to the load.

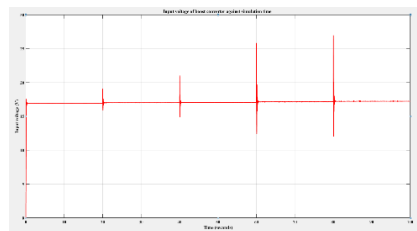


Figure 11: The graph of input DC-link voltage against simulation time

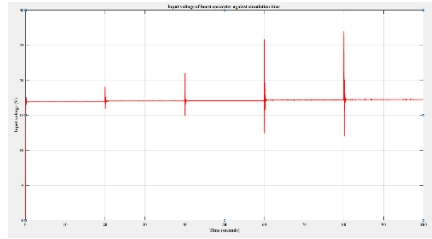


Figure 12: The graph of output DC-link voltage against simulation time

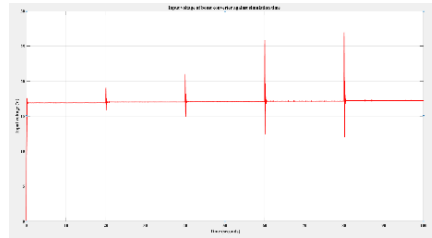


Figure 13: The graph of output current against simulation time

3.4 State-of-charge (SOC), current, voltage of lead-acid battery and duty cycle (charging process)

During the simulation, the BDC of VAWEHS is operated in buck mode in default. The SOC, current and voltage across the lead-acid battery are observed and plotted as Figure 14, Figure 15 and Figure 16, respectively. Based on Figure 14, the SOC of lead-acid battery is increased with time. This indicates that the lead-acid battery is charged in the proposed VAWEHS. This evidence is supported by Figure 16 that shows a graph plotted with negative value of current. This is because the negative current of battery indicates that there is a current flow from the BDC to the lead-acid battery. From Figure 16, due to the highly charges input capacitor of the boost converter, the lead-acid battery is able to receive a portion of current for the charging purpose. Current of 184.5 A is recorded as the highest amount of charging current transferred to battery when the wind speed is 6.667 m/s. Besides, negative value can be found in Figure 15 as the current flow from BDC to lead-acid battery so that the battery can be charged. Figure 16 shows the graph of voltage of battery against the simulation time. From that figure, the lead-acid battery is charged across the voltage from 8.2 V to 11.5 V from the simulation time of 0 to 80 seconds. When the time is more than 80 seconds, the voltage exceeds 12 V which is the nominal voltage of lead-acid battery. AT this instance, the charging process is very efficient and there is a sharp increase in SOC after 80 seconds.

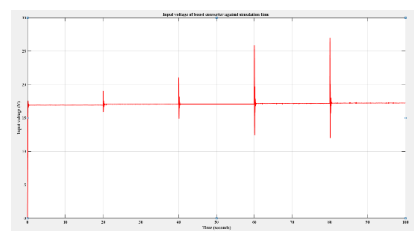


Figure 14: The graph of SOC of battery against simulation time during charging process

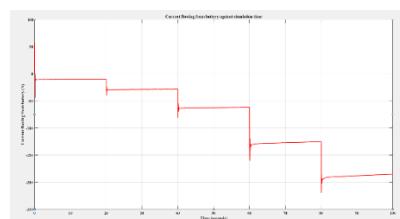


Figure 15: The graph of current of battery against simulation time during charging process

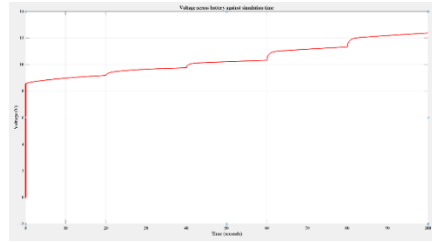


Figure 16: The graph of voltage across battery against simulation time during charging process

3.5 State-of-charge, current, and voltage of lead-acid battery (discharging process)

Figure 17 and Figure 18 show the graphs of current and voltage of battery during the discharging process, respectively. During the simulation, the speed of wind is set to 0 m/s so that the BDC will be operated in boost mode. From Figure 18, positive value of current is recorded during the simulation. This indicates that current is flowing from the lead-acid battery to the system, and this phenomenon can only be occurred in discharging process. The current is stabled from an extremely high value to the range of 0 A to 7 A after a very short time due to the switching process of switching device in BDC. From Figure 19, the lead-acid battery supplies energy to the load at its nominal voltage, which is 12 V.

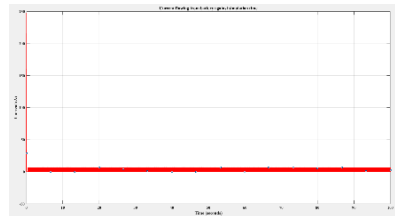


Figure 17: The graph of current of battery against simulation time during discharging process

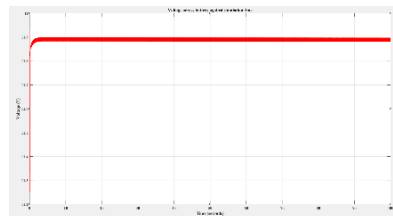


Figure 18: The graph of battery of battery against simulation time during discharging process

3.6 Output voltage and output current of the boost converter (discharging process)

Figure 19 and Figure 20 show the graphs of output voltage and current of boost converter during the discharging process, respectively. From both figures, the boost converter is capable to supply a current of 1.7 A at the output voltage of 18.5 V across the load of 10.8 Ω when 0 m/s of wind speed is detected by the system. This evidence show that the lead-acid battery is able to discharge to supply electricity to the load. The output current and output voltage are stabilised from a very high value to 18.5 V and 1.7 A, respectively due to the DC-link voltage control scheme that is applied to BDC.

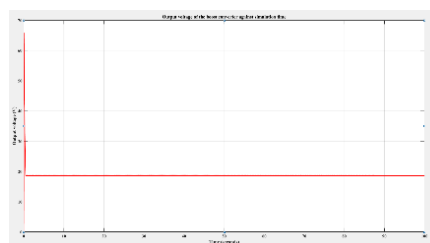


Figure 19: The graph of output voltage against simulation time during discharging process

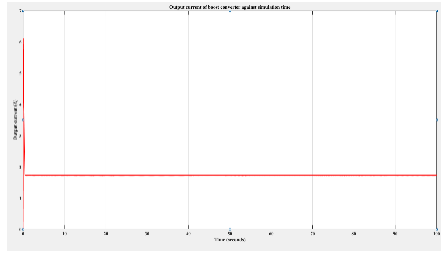


Figure 20: The graph of output current against simulation time during discharging process

4. Conclusion

Overall, in this project, the proposed VAWEHS can perform well in harnessing wind energy to generate electrical energy under the wind speeds of 1.667 m/s, 2.500 m/s, 3.611 m/s, 5.278 m/s and 6.667 m/s. The system is capable to produce the desired voltage level of 18.5 V across a 10.8 Ω load with the aid of the DC-link voltage control scheme. The system is capable of supplying a current of 1.7 A to the load. The system is also able to store the electrical energy generated into a lead-acid battery when the bidirectional converter is operated in buck mode. The highest current that can be received during the charging process is 185.4 A. This system is also capable to supply a current of 1.7 A across the voltage of 18.5 V to the load with the help of boost converter during the discharging process. However, this portable VAWEHS can be improved further so that its performance can be enhanced. To overcome this, advanced control scheme such as maximum power point tracking (MPPT) is recommended to be introduced to maximise the energy available from the connected VAWT.

Acknowledgement

The authors would like to thank the Faculty of Electrical and Electronic Engineering, Universiti Tun Hussein Onn Malaysia for its support.

References

- [1] K. Tromly, "Renewable Energy: An Overview. Energy Efficiency and Renewable Energy Clearinghouse (EREC) Brochure."
- [2] Energy Commission (Malaysia), "Energy Malaysia: Smarter Consumers," *Energy Malaysia*, vol. 11, p. 27, 2017, Accessed: Oct. 12, 2021. [Online]. Available: www.st.gov.my
- [3] Asia Wind Energy Association, "Malaysia – Asia Wind Energy Association 2020," *Asia Wind Energy Association*. 2020, Accessed: Oct. 22, 2020. [Online]. Available: <https://www.asiawind.org/research-data/market-overview/malaysia/>
- [4] M. Cheang, "Pulau Perhentian Kecil now powered by the sun and wind - Community | The Star Online," *The Star Online*, 2007. <https://www.thestar.com.my/news/community/2007/09/25/pulau-perhentian-kecil-now-powered-by-the-sun-and-wind> (accessed Jul. 01, 2021)
- [5] B. O. Omijeh, C. S. Nmom, and E. Nlewem, "Modeling of a Vertical Axis Wind Turbine with Permanent Magnet Synchronous Generator for Nigeria," *Int. J. Eng. Technol. Vol.*, vol. 3, no. 2, pp. 212–220, 2013
- [6] K. A. Sunny and N. M. Kumar, "Vertical Axis Wind Turbine: Aerodynamic Modelling and its Testing in Wind Tunnel," *Procedia Comput. Sci.*, vol. 93, no. September, pp. 1017–1023, 2016, doi: 10.1016/j.procs.2016.07.305

- [7] A. M. Eid, M. Abdel-Salam, and M. T. Abdel-Rahman, "Vertical-axis wind turbine modeling and performance with axial-flux permanent magnet synchronous generator for battery charging applications," *Proc. 11th Int. Middle East Power Syst. Conf. MEPCON'2006*, vol. 1, no. December 2006, pp. 162–166, 2006
- [8] A. Russakoff, "Calculator Calculations," *Math. Teach.*, vol. 72, no. 3, p. 188, 2021, doi: 10.5951/mt.72.3.0188